

Electronic structure and spin-orbit coupling in ternary transition metal chalcogenides Cu_2TlX_2 (X = Se, Te)

Na Qin(秦娜), Xian Du(杜宪), Yangyang Lv(吕洋洋), Lu Kang(康璐), Zhongxu Yin(尹中旭), Jingsong Zhou(周景松),Xu Gu(顾旭), Qinqin Zhang(张琴琴), Runzhe Xu(许润哲), Wenxuan Zhao(赵文轩), Yidian Li(李义典),Shuhua Yao(姚淑华), Yanfeng Chen(陈延峰), Zhongkai Liu(柳仲楷),Lexian Yang(杨乐仙), and Yulin Chen(陈宇林)
Citation: Chin. Phys. B, 2022, 31 (**3**): 037101. DOI: 10.1088/1674-1056/ac3ecd
Journal homepage: http://cpb.iphy.ac.cn; http://iopscience.iop.org/cpb

What follows is a list of articles you may be interested in

$SU(3)$ spin-orbit coupled fermions in an optical lattice

Xiaofan Zhou(周晓凡), Gang Chen(陈刚), and Suo-Tang Jia(贾锁堂)
Chin. Phys. B, 2022, 31 (**1**): 017102. DOI: 10.1088/1674-1056/ac11dc

Influence of thickness on current-induced magnetization switching in $L1_0$-FePt single layer

Shi-Qi Zheng(郑诗琪), Kang-Kang Meng(孟康康), Zhen-Guo Fu(付振国), Ji-Kun Chen(陈吉堃), Jun Miao(苗君), Xiao-Guang Xu(徐晓光), and Yong Jiang(姜勇)
Chin. Phys. B, 2021, 30 (**10**): 107101. DOI: 10.1088/1674-1056/ac0a62

Magnetic impurity in hybrid and type-II nodal line semimetals

Xiao-Rong Yang(杨晓容), Zhen-Zhen Huang(黄真真), Wan-Sheng Wang(王万胜), and Jin-Hua Sun(孙金华)
Chin. Phys. B, 2021, 30 (**6**): 067103. DOI: 10.1088/1674-1056/abfa02

Two-dimensional hexagonal Zn_3Si_2 monolayer: Dirac cone material and Dirac half-metallic manipulation

Yurou Guan(官雨柔), Lingling Song(宋玲玲), Hui Zhao(赵慧), Renjun Du(杜仁君), Liming Liu(刘力铭), Cuixia Yan(闫翠霞), Jinming Cai(蔡金明)
Chin. Phys. B, 2020, 29 (**8**): 087103. DOI: 10.1088/1674-1056/ab943a

Giant interface spin-orbit torque in NiFe/Pt bilayers

Shu-Fa Li(李树发), Tao Zhu(朱涛)
Chin. Phys. B, 2020, 29 (**8**): 087102. DOI: 10.1088/1674-1056/ab9292

RAPID COMMUNICATION

Electronic structure and spin–orbit coupling in ternary transition metal chalcogenides Cu_2TlX_2 (X = Se, Te)

Na Qin(秦娜)[1], Xian Du(杜宪)[1], Yangyang Lv(吕洋洋)[2], Lu Kang(康璐)[1], Zhongxu Yin(尹中旭)[1], Jingsong Zhou(周景松)[1], Xu Gu(顾旭)[1], Qinqin Zhang(张琴琴)[1], Runzhe Xu(许润哲)[1], Wenxuan Zhao(赵文轩)[1], Yidian Li(李义典)[1], Shuhua Yao(姚淑华)[2], Yanfeng Chen(陈延峰)[2], Zhongkai Liu(柳仲楷)[3,4], Lexian Yang(杨乐仙)[1,5], and Yulin Chen(陈宇林)[1,3,4,6,†]

[1] *State Key Laboratory of Low Dimensional Quantum Physics, Department of Physics, Tsinghua University, Beijing* 100084, *China*
[2] *National Laboratory of Solid State Microstructures, Department of Materials Science and Engineering, Nanjing University, Nanjing* 210093, *China*
[3] *School of Physical Science and Technology, ShanghaiTech University and CAS–Shanghai Science Research Center, Shanghai* 201210, *China*
[4] *ShanghaiTech Laboratory for Topological Physics, Shanghai* 200031, *China*
[5] *Frontier Science Center for Quantum Information, Beijing* 100084, *China*
[6] *Department of Physics, Clarendon Laboratory, University of Oxford, Parks Road, Oxford OX*1 3*PU, UK*

(Received 28 August 2021; revised manuscript received 26 October 2021; accepted manuscript online 1 December 2021)

Ternary transition metal chalcogenides provide a rich platform to search and study intriguing electronic properties. Using angle-resolved photoemission spectroscopy and *ab initio* calculation, we investigate the electronic structure of Cu_2TlX_2 (X = Se, Te), ternary transition metal chalcogenides with quasi-two-dimensional crystal structure. The band dispersions near the Fermi level are mainly contributed by the Te/Se p orbitals. According to our *ab-initio* calculation, the electronic structure changes from a semiconductor with indirect band gap in Cu_2TlSe_2 to a semimetal in Cu_2TlTe_2, suggesting a band-gap tunability with the composition of Se and Te. By comparing ARPES experimental data with the calculated results, we identify strong modulation of the band structure by spin–orbit coupling in the compounds. Our results provide a ternary platform to study and engineer the electronic properties of transition metal chalcogenides related to large spin–orbit coupling.

Keywords: transition metal chalcogenides, spin–orbit coupling, electronic structure, angle-resolved photoemission spectroscopy (ARPES)

PACS: 71.70.Ej, 71.20.−b, 71.20.Nr **DOI:** 10.1088/1674-1056/ac3ecd

1. Introduction

Transition metal chalcogenides with quasi-two-dimensional crystal structure exhibit various fascinating properties, such as superconductivity, charge-density wave, magnetism, novel topological phase, valleytronics, etc.,[1–14] which provide not only significant scientific implications but also great application potential in the next-generation electronic and spintronic devices. Recently, ternary transition metal chalcogenides (TTMCs) have attracted great attention. Compared with their binary counterparts, TTMCs show improved tunability and complexity, thus promising a rich platform to search for and study new physics, such as the interplay between magnetism and topology, giant anomalous Hall effect, and topological quantum properties.[15–21]

It is well-known that spin–orbit coupling (SOC) plays a pivotal role in the novel properties of quantum materials. It serves as a fundamental tuning parameter to bridge different topological phases;[22–25] it is also essentially related to the large magnetoresistance[26] and magnetocrystalline anisotropy[27] in solid materials; from application perspective, it enables electrical manipulation of spins, which is of significant importance in the newly developed spintronics and valleytronics. Therefore, it is attractive to search for and investigate materials with large SOC.

In this work, using high-resolution angle-resolved photoemission spectroscopy (ARPES) and *ab initio* calculation, we study the electronic structures of Cu_2TlTe_2 and Cu_2TlSe_2, newly discovered ternary transition metal chalcogenides. Our calculation shows a semiconductor and semimetal phase in Cu_2TlTe_2 and Cu_2TlSe_2, respectively, suggesting a tunability of the band gap with Se/Te composition. The band dispersions near the Fermi level (E_F) are mainly from p orbitals, that is, 5p orbitals of Te and 4p orbitals of Se. With the help of *ab initio* calculation, we identify strong SOC effect that lifts the band degeneracy and opens large energy gaps in the band structure. Moreover, we observe a band folding near the X point, suggesting a surface reconstruction or surface charge-density wave. Our study provides insights into the SOC and electronic structure of TTMC materials Cu_2TlX_2, which may be an interesting and useful platform to search and study novel physics, particularly in their ultrathin films.

†Corresponding author. E-mail: yulin.chen@physics.ox.ac.uk

© 2022 Chinese Physical Society and IOP Publishing Ltd

2. Methods

High-quality Cu_2TlX_2 crystals were synthesized using Bridgeman method.[28] ARPES measurements were performed at beam line I05 of the Diamond Light Source (DLS, proposal No. SI20683-1), beam line 13U of the National Synchrotron Radiation Laboratory (NSRL), and Tsinghua University. Scienta R4000 (DA30) analyzer was used at DLS (NSRL). Measurements at Tsinghua University were performed using DA30L analyzer and VUV5050 helium lamp. Samples were cleaved and measured under ultrahigh vacuum better than 1×10^{-10} mbar. The overall energy and angular resolutions were 15 meV and 0.2°, respectively. First-principles band structure calculations of Cu_2TlX_2 (X = Se, Te) were performed using QUANTUM ESPRESSO code package[29] with a plane wave basis. The pseudopotentials suggested by Standard Solid State Pseudopotentials (SSSP) Precision v1.1[30] were chosen for all elements. The exchange and correlation energy was considered under Perdew–Burke–Ernzerhof (PBE) type generalized gradient approximation (GGA).[31] Both lattice constants and fractional atomic coordinates were set to the experimental values. The cutoff energy for the plane-wave basis was set to 560 eV in all calculations, which was sufficient to converge the total energy for a given k-point sampling. A Γ-centered Monkhorst–Pack k-point mesh of $16 \times 16 \times 16$ ($15 \times 15 \times 15$) with a spacing of 0.15 Å^{-1} was adopted for Cu_2TlSe_2 (Cu_2TlTe_2) to get a self-consistent charge density. Both the conditions of excluding and including spin–orbit coupling were considered in the self-consistent calculations. The electronic minimization algorithm used for self-consistent calculations was a blocked Davidson algorithm. Surface-projected band structures were calculated with the WANNIERTOOLS package,[32] based on the tight-binding type Hamiltonian constructed from maximally localized Wannier functions (MLWF) supplied by the Wannier90 code,[33] by projecting the *ab initio* constructed (Kohn–Sham) Bloch states into the atomic-orbital like Wannier functions starting from a $9 \times 9 \times 9$ uniform k grid.

3. Results and discussion

Copper based ternary TTMCs Cu_2TlX_2 (X = Se, Te) crystallize into a layered tetragonal $ThCr_2Si_2$-type structure with alternatively stacking Cu_2X_2 and Tl layers, as shown in Fig. 1(a). Figure 1(b) shows the three-dimensional Brillouin zone of Cu_2TlX_2 and its surface projection with high-symmetry points indicated. Our resistivity measurements in Fig. 1(c) show prototypical metallic behaviors that can be well understood within Fermi-liquid theory.[28] We observe sharp peaks in single crystal x-ray diffraction measurements, suggesting a lattice constant of c = 14.03 Å and 15.21 Å for Cu_2TlSe_2 and Cu_2TlTe_2, respectively.

Although the materials are quasi-two dimensional, our photon-energy dependent Fermi surface (FS) measurements on Cu_2TlTe_2 in Fig. 2(a) show resolvable variation. Using an inner potential of 13 eV, we can determine the high symmetry points along k_z, as shown in Figs. 2(a) and 2(b). We observe a strong dispersion between −0.95 eV and −0.5 eV along ΓZ [white dashed line in Fig. 2(b)], suggesting an important role of interlayer coupling in the electronic structure of Cu_2TlTe_2. The Γ and Z points can be approached by 122 eV and 102 eV photons, respectively. Figures 2(c) and 2(d) show the evolution of the constant energy contour with binding energy on the $\Gamma\Sigma X$ and $Z\Sigma_1Y_1$ planes, respectively. The measured Fermi surface consists of a four-fold symmetric hole pocket near the $\bar{\Gamma}$ point, an electron pocket around the $\bar{M}$ point, and a small hole pocket around the $\bar{X}$ point, which evolves into a complex texture at high binding energies. The FS and constant energy contours at different binding energies are perfectly reproduced by our *ab initio* calculation as shown in Fig. 2(e).

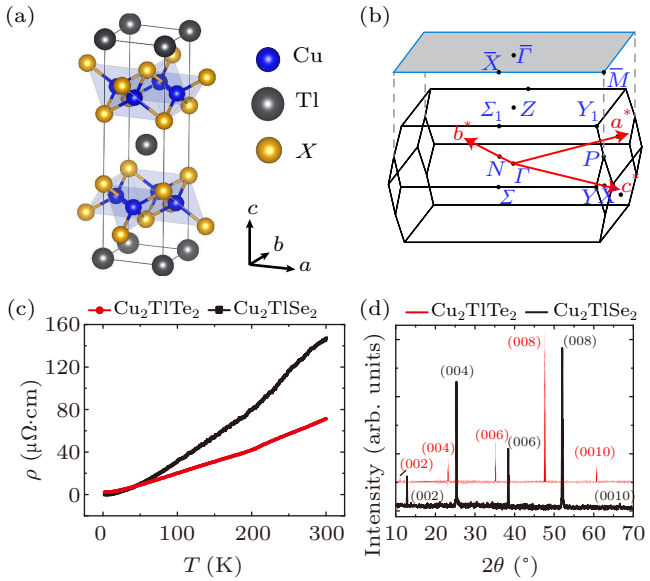


Fig. 1. (a) Crystal structure of Cu_2TlX_2 (X = Se, Te). (b) Three-dimensional Brillouin zone of Cu_2TlX_2 and its surface projection with high-symmetry points indicated. (c) Resistivity of Cu_2TlX_2 as a function of temperature. (d) Single-crystal x-ray diffraction data of Cu_2TlSe_2 and Cu_2TlTe_2.

Figure 3 shows the band structure of Cu_2TlTe_2 along high symmetry directions. We observe anisotropic dispersions along $\Gamma\Sigma$ and ΓX [Figs. 3(a)–3(c)]. Near E_F, there exist mainly two bands, α and β crossing E_F. The α band is nearly flat near the Γ point, which may contribute high density of states near E_F. The β band, on the other hand, shows a linear dispersion in a large energy range, as shown in Figs. 3(b) and 3(c). The Fermi velocity of the β band is about 4.8 eV·Å along ΣX, about 60% of that of graphene.[16] The linear dispersion of the β band may contribute to the unsaturated magnetoresistance in Cu_2TlTe_2 at high magnetic field.[28] The band structure of Cu_2TlTe_2 is nicely reproduced by our calculation with SOC included [Figs. 3(d) and 3(e)], in which the α and β bands are shown by the blue and red curves, respectively. We emphasize that the k_z dispersion observed in Fig. 2(b) is also captured by our *ab initio* calculation.

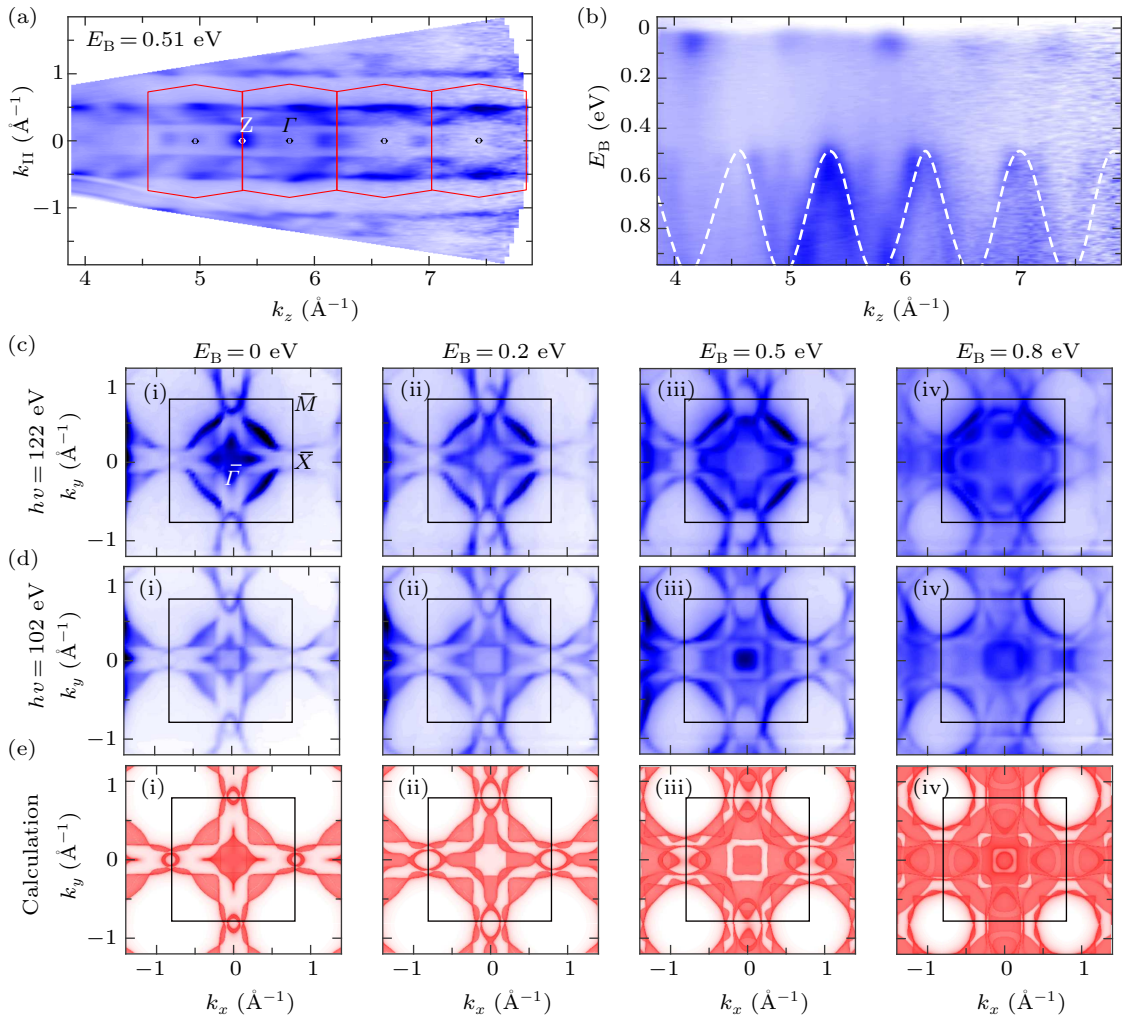


Fig. 2. (a) Fermi surface of Cu_2TlTe_2 in the $\Gamma\Sigma Z$ plane obtained by photon-energy dependent measurements. (b) The k_z-dispersion along ΓZ. (c), (d) Evolution of the constant-energy-contours with binding energy on (c) $\Gamma\Sigma X$ and (d) $Z\Sigma_1 Y_1$ planes, respectively. (e) Calculated constant-energy-contours of Cu_2TlTe_2. Data were taken at 10 K.

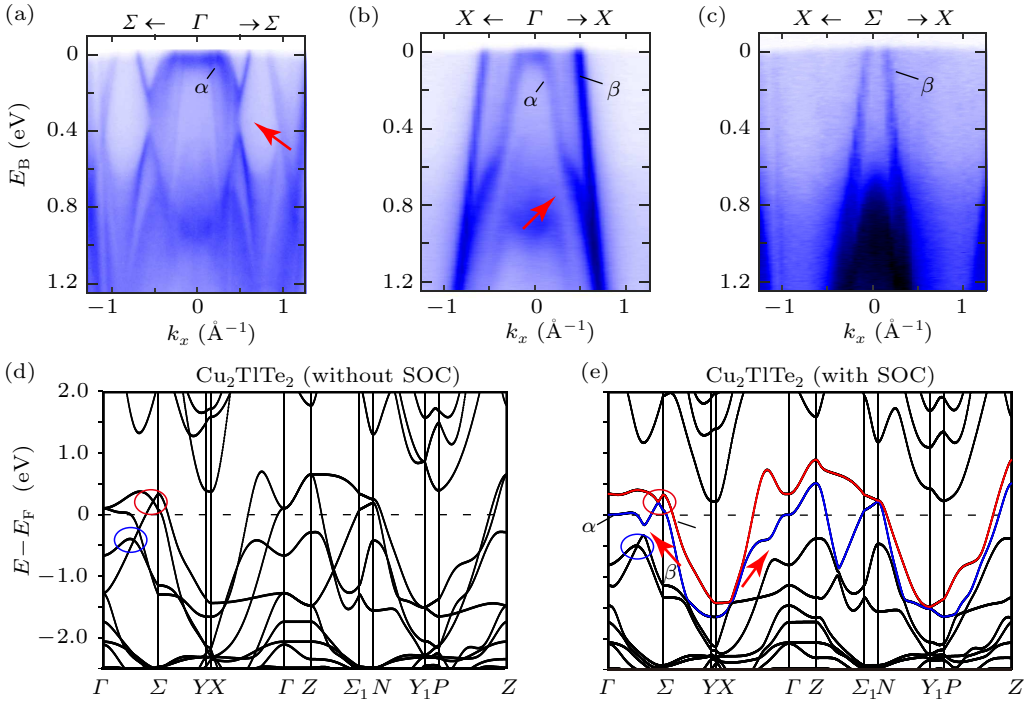


Fig. 3. (a)–(c) ARPES measured band dispersions of Cu_2TlTe_2 along high symmetry directions. (d), (e) Band structures obtained by *ab initio* calculation with (d) and without (e) spin–orbit coupling (SOC). The red arrows indicate the band gaps induced by SOC. The red and blue circles indicate the band crossings with small energy gap. Data were taken with 122 eV photons at 10 K.

By comparing our experiment with the calculations with and without SOC, we notice that the flat band near Γ is actually induced by the strong SOC in the system. Moreover, the SOC induces a band gap as large as 399 (174) meV along the ΓX ($\Gamma\Sigma$) direction [red arrows in Fig. 3(e)], in good agreement with our experiment [red arrows in Figs. 3(a) and 3(b)], suggesting strong SOC effect modulating the band structure of Cu_2TlTe_2. The SOC also lifts the band degeneracy along ΓZ, inducing a band splitting as large as 380 meV.

Figure 4 shows the band structure of Cu_2TlSe_2. Overall, the band structure of Cu_2TlSe_2 is very similar to that of Cu_2TlTe_2. The Fermi surface is likewise mainly contributed by the α and β bands [Fig. 4(a)]. The flat band near E_F as in Cu_2TlTe_2 is not observed since it locates slightly above E_F, and such difference may be due to the non-stoichiometry of Cu_2TlTe_2.[28] However, we observe another flat band near 500 meV below E_F using 21.2 eV photons [Figs. 4(b) and 4(c)]. The Fermi velocity of the β band along $\bar{\Sigma}\bar{X}$ is about 2 eV·Å, much smaller than that in Cu_2TlTe_2. The band gap along $\bar{\Gamma}\bar{X}$ [red arrows in Figs. 4(c) and 4(f)] and the band splitting along ΓZ induced by SOC are also much smaller than those in Cu_2TlTe_2, suggesting a stronger SOC effect in Cu_2TlTe_2. The measured band structure of Cu_2TlSe_2 and calculations along high symmetry directions are shown in Figs. 4(b)–4(f). Although the flat band near -500 meV is not in the calculation along high symmetry points, it can be reproduced by the calculation at a k_z position between Γ and Z, since the band below the α band shows an electron (hole) like dispersion along $\Gamma\Sigma$ ($Z\Sigma_1$) in the calculation [Fig. 4(f)]. Indeed, the k_z value corresponding to 21.2 eV photons is estimated to be near the middle of Γ and Z in the Brillouin zone.

From the calculations in Figs. 3(e) and 4(f), we note that Cu_2TlSe_2 is a semiconductor with indirect band gap of about 226 meV, in contrast to the semi-metallic band structure of Cu_2TlTe_2, suggesting a tunability of the band gap by Se/Te composition in the Cu_2TlX_2 materials. We further conducted orbital-projected *ab-initio* calculation as shown in Fig. 5. The band dispersions near E_F are mainly contributed by the 4p/5p orbital of the Se/Te atoms. Therefore, the change of Se/Te composition can efficiently tune the band gap of Cu_2TlX_2. It is worth noting that both of our Cu_2TlX_2 samples are p-doped with the valence bands crossing E_F. Further electron doping or the synthesis of intrinsic samples are required to establish the tunability of the band gap.

In both Cu_2TlTe_2 and Cu_2TlSe_2, there exist band crossings that are nearly gapless along $\Gamma\Sigma$ [red and blue circles in Figs. 3(d), 3(e), 4(e) and 4(f)]. According to our calculation, the hybridization gaps near these band crossings are less than 10 meV in Cu_2TlTe_2 and less than 5 meV in Cu_2TlSe_2, which are immune to the SOC [red and blue circles in Figs. 3(d), 3(e), 4(e) and 4(f)]. In Cu_2TlSe_2, we observe a Dirac-like band dispersion near E_F, consistent with our calculation [red circles in Figs. 4(b) and 4(f)]. It is likely that, with lighter atoms in the system, for example, in Cu_2TlS_2, a nearly gapless Dirac fermion can exist near E_F.

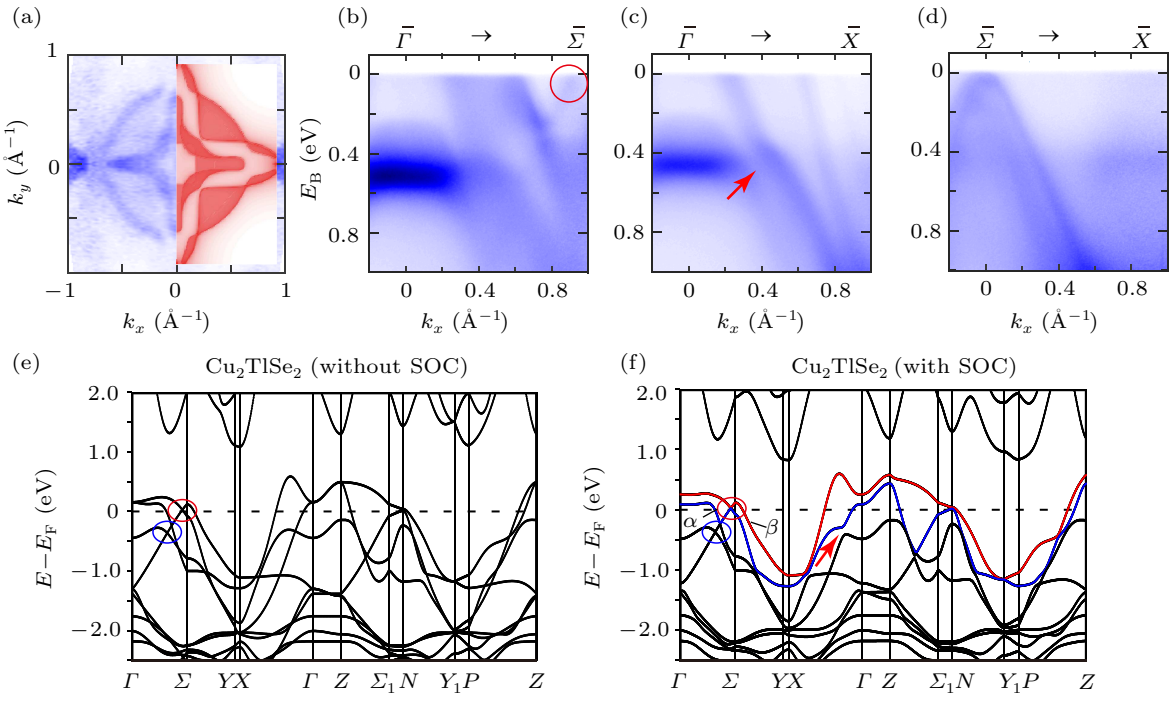


Fig. 4. (a) Measured (left) and calculated (right) Fermi surface of Cu_2TlSe_2. (b)–(d) ARPES measured band dispersions of Cu_2TlSe_2 along high symmetry directions. (e), (f) Band structure obtained by *ab initio* calculation with (e) and without (f) SOC. The red arrows indicate the band gaps induced by SOC. The red and blue circles indicate the band crossings with small energy gap. Data were collected with 21.2 eV photons delivered by a helium lamp at 68 K.

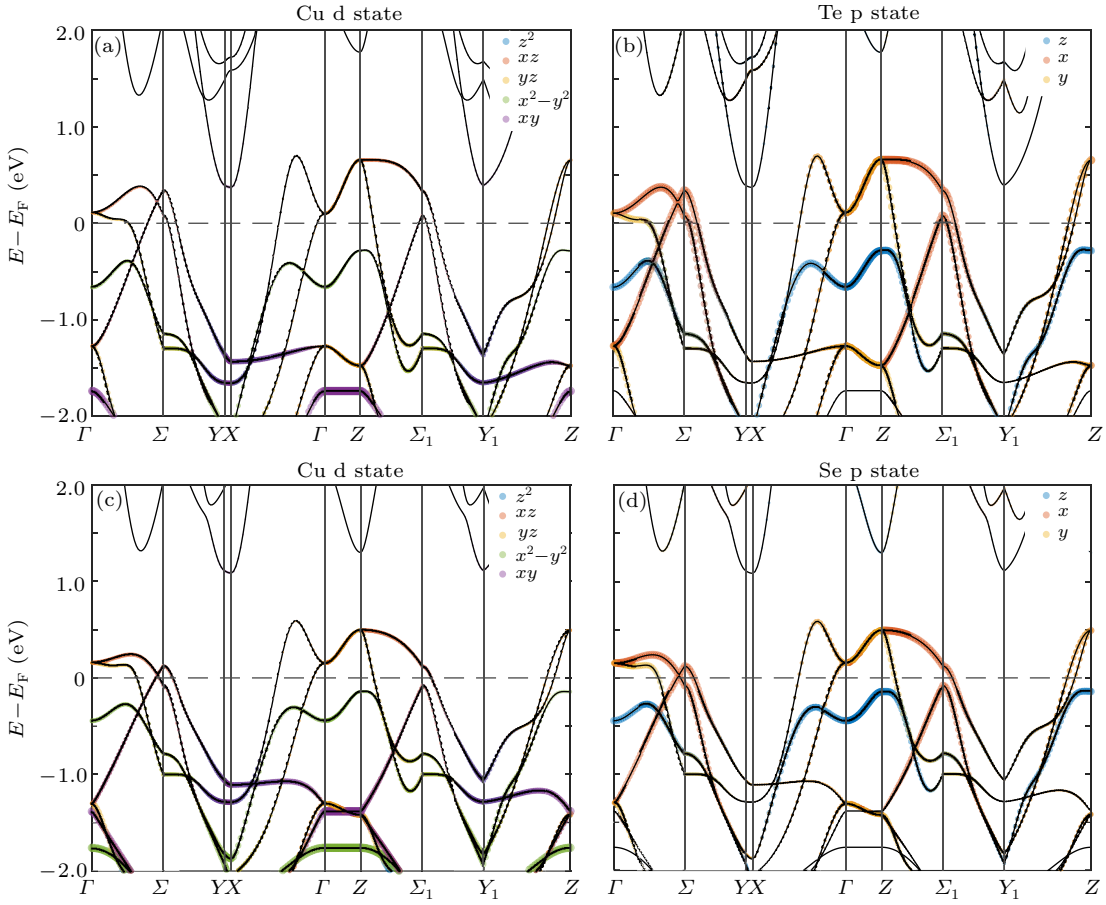


Fig. 5. Orbital-projected band structure calculations of Cu_2TlX_2 without SOC, in which the point size indicates the weight of the orbital contributions to band dispersions. (a), (b) Cu d and Te p states in Cu_2TlTe_2. (c), (d) Cu d and Se p states in Cu_2TlSe_2.

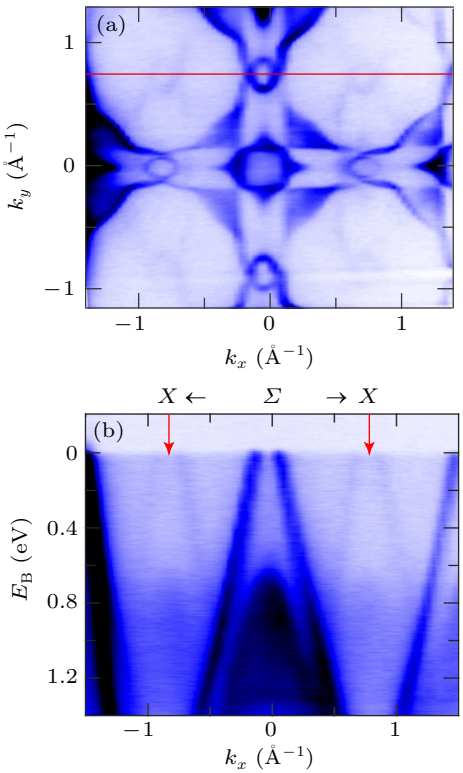


Fig. 6. (a) Fermi surface of Cu_2TlTe_2 measured with 80 eV photon energy. (b) Band dispersion of Cu_2TlTe_2 along ΣX, which is indicated by red line in (a), showing band folding from the Σ point to the X point. Data were collected at 10 K.

Noticeably, in the Fermi surface and band dispersion along ΣX of Cu_2TlTe_2, we observe band folding from Σ to X (Figs. 6(a) and 6(b)) using photon energy of 80 eV that is more surface-sensitive. The band folding from Σ to Γ is also resolvable in Fig. 3(a), which complicates the band dispersion near Γ in Fig. 3(a). Such band folding suggests a 2-fold reconstruction of the crystal structure. Since we do not observe any anomaly in temperature dependent resistivity measurements, the observed band folding is likely due to a surface reconstruction or surface charge-density wave, which requires further experimental investigations.

4. Summary

To sum up, we systematically measure the electronic structure of Cu_2TlX_2 using high-resolution ARPES. The transition from a semiconductor in Cu_2TlSe_2 to a semimetal in Cu_2TlTe_2, as indicated by our *ab initio* calculation, suggests a tunability of the electronic structure and physical property of the materials with Se/Te composition. With the help of *ab initio* calculation, we identify strong SOC effect in the band structure of Cu_2TlTe_2, which opens a band gap and lifts the band degeneracy along ΓZ. We propose that a massless Dirac fermion may exist near E_F in the sibling Cu_2TlX_2 crystal, i.e.,

Cu_2TlS_2 if it is successfully synthesized. Our results are helpful to understand the electronic properties of Cu_2TlX_2, and also provide a material platform to search for SOC-related physics.

Acknowledgments

This study was supported by the National Natural Science Foundation of China (Grant No. 11774190). We thank for access to DLS beamline I05 and NSRL beamline 13U with help from S. W. Jung, C. Cacho, S. T. Cui, and Z. Sun.

References

[1] Manzeli S, Ovchinnikov D, Pasquier D, Yazyev OV and Kis A 2017 *Nat. Rev. Mater.* **2** 17033
[2] Wang G, Chernikov A, Glazov M, Heinz T, Marie X, Amand T and Urbaszek 2018 *Rev. Mod. Phys.* **90** 021001
[3] Klemm R A 2015 *Physica C* **514** 86
[4] Morosan E, Zandbergen H W, Dennis B S, Bos J W G, Onose Y, Klimczuk T, Ramirez A P, Ong N P and Cava R J 2006 *Nat. Phys.* **2** 544
[5] Sipos B, Kusmartseva A F, Akrap A, Berger H, Forró L and Tutiš E 2008 *Nat. Mater.* **7** 960
[6] Qian X, Liu J, Fu L and Li J 2014 *Science* **346** 1344
[7] Zhang Q H, Liu Z K, Sun Y, Yang H F, Jiang J, Mo S K, Hussain Z, Qian X F, Fu L, Yao S H, Lu M H, Felser C, Yan B H, Chen Y L and Yang L X 2017 *Physica Status Solidi (RRL)–Rapid Research Letters* **11** 1700209
[8] Jiang J, Liu Z K, Sun Y, Yang H F, Rajamathi C R, Qi Y P, Yang L X, Chen C, Peng H, Hwang C C, Sun S Z, Mo S K, Vobornik I, Fujii J, Parkin S S P, Felser C, Yan B H and Chen Y L 2017 *Nat. Commun.* **8** 13973
[9] Rossnagel K 2011 *J. Phys: Condens Matter.* **23** 213001
[10] Xu X, Yao W, Xiao D and Heinz T F 2014 *Nat. Phys.* **10** 343
[11] Wilson J A and Yoffe A D 1969 *Adv. Phys.* **18** 193
[12] Mak K F, McGill K L, Park J and McEuen P L 2014 *Science* **344** 1489
[13] Fang Y Q, Pan J, Zhang D Q, Wang D, Hirose H T, Terashima T, Uji S, Yuan Y H, Li W, Tian Z, Xue J M, Ma Y H, Zhao W, Xue Q K, Mu G, Zhang H J and Huang F Q 2019 *Adv. Mater.* **31** 1901942
[14] Mok B H, Rao S M, Ling M C, Wang K J, Ke C T, Wu P M, Chen C L, Hsu F C, Huang T W, Luo J Y, Yan D C, Ye K W, Wu T N, Chang A M and Wu M K 2009 *Crystal Growth & Design.* **9** 3260
[15] Chen Y J, Xu L X, Li H J, Li Y W, Wang H Y, Zhang C F, Li H, Wu Y, Liang A J, Chen C, Jung S W, Cacho C, Mao Y H, Liu S, Wang M X, Guo Y F, Xu Y, Liu Z K, Yang L X and Chen Y L 2019 *Phys. Rev. X* **9** 041040
[16] Sprinkle M, Siegel D, Hu Y, Hicks J, Tejeda A, Taleb-Ibrahimi A, Le Fèvre P, Bertran F, Vizzini S, Enriquez H, Chiang S, Soukiassian P, Berger C, de Heer W A, Lanzara A and Conrad E H 2019 *Phys. Rev. Lett.* **103** 226803
[17] Hao Y J, Liu P F, Feng Y, *et al.* 2019 *Phys. Rev. X* **9** 041038
[18] Li H, Gao S Y, Duan S F, *et al.* 2019 *Phys. Rev. X* **9** 041039
[19] Kim K, Seo J, Lee E, Ko K T, Kim B S, Jang B G, Ok J M, Lee J, Jo Y J, Kang W, Shim J H, Kim C, Yeom H W, Min B I, Yang B J and Kim J S 2018 *Nat. Mater.* **17** 794
[20] Liu E, Sun Y, Kumar N, *et al.* 2018 *Nat. Phys.* **14** 1125
[21] Liu D F, Liang A J, Liu E K, *et al.* 2019 *Science* **365** 1282
[22] Qi X L and Zhang S C 2011 *Rev. Mod. Phys.* **83** 1057
[23] Hasan M Z and Kane C L 2010 *Rev. Mod. Phys.* **82** 3045
[24] Chen Y J, Gu X, Li Y D, Du X, Yang L X and Chen Y L 2020 *Matter* **3** 1114
[25] Lv B, Qian T and Ding H 2019 *Nature Reviews Physics* **1** 609
[26] Jiang J, Tang F, Pan X C, *et al.* 2015 *Phys. Rev. Lett.* **115** 166601
[27] Van Vleck J H 1937 *Phys. Rev.* **52** 1178
[28] Li X, Lv Y Y, Pang B, Zhang B B, Cao L, Yao S H, Zhou J, Chen Y B, Dong S T, Zhang S T, Lu M H and Chen Y F 2017 *Mater. Res. Bull.* **89** 97
[29] Giannozzi P, Baroni S, Bonini N, *et al.* 2009 *J. Phys. Condens. Matter.* **21** 395502
[30] Prandini G, Marrazzo A, Castelli I E, Mounet N and Marzari N 2018 *NPJ Computational Materials* **4** 72
[31] Perdew J P, Burke K and Ernzerhof M 1996 *Phys. Rev. Lett.* **77** 3865
[32] Wu Q, Zhang S, Song H F, Troyer M and Soluyanov A A 2018 *Computer Physics Communications* **224** 405
[33] Mostofi A A, Yates J R, Lee Y S, Souza I, Vanderbilt D and Marzari N 2008 *Computer Physics Communications* **178** 685